To determine the onset of motor dysfunction in transgenic mice, we adopted a balance beam test using the stainless steel bar (500 mm long and 9 mm in diameter). We assessed motor function in the hind limbs at 12 weeks of age, and thereafter until the mice were unable to stay on the bar. We used the following five arbitrary scales to evaluate the motor function of mice; Grade 5 (swift walking and change of directions on bar without hind limb slipping), Grade 4 (walking but with occasional hind limb slipping), Grade 3 (walking awkwardly with frequent hind limb slipping), Grade 2 (crawls few steps and falls off), and Grade 1 (unable to stay on bar). In this study, the Grade 3 was defined as the sign of the disease onset.

We commenced the daily administration of the compound(s) for mice that showed signs of motor dysfunction (deemed age of onset) between 121 days and 130 days, and continued until their terminal phase (death).

Pharmacokinetics of BRC in mice

Wild type mice at 12 weeks of age (male, C57BL/6N) were used for the analysis of BRC pharmacokinetics. BRC suspended with 0.5% CMC-Na were injected intraperitoneally at a dose of 10 mg/5 ml/kg body weight. After 5 min, 15 min, 30 min, 1 h, 2 h, and 4 h, we draw the blood samples from anethesized animals, thereafter transcardially perfused with physiological saline containing 10% heparin under anesthesia, and excised the whole brain. Each blood sample was centrifuged at 1000×*g* for 10 min at 4 °C, and serum fraction was collected. The brain was frozen in liquid nitrogen, and was cryopreserved until used.

We mixed serum with deproteinization buffer (0.05 M H_2SO_4, 2.5 M K_2CO_3, and diethylester), and collected organic layer after centrifugation at 1500×*g* for 10 min. Organic layer was mixed with 0.05 M H_2SO_4, and then collected water layer after centrifugation at 1500×*g* for 10 min. After the addition of methanol, each sample solution from serum was subjected to HPLC.

Mouse whole brain was homogenized with acetonitrile and left at −80 °C for 10 min. The supernatant was collected after centrifugation at 10,000×*g* for 10 min at 4 °C and was dried under vacuum. The dried sample was re-dissolved in methanol and mixed with two volumes of 10 mM phosphate buffer (pH 7.0), and then the supernatant was collected by centrifugation at 10,000×*g* for 10 min at 4 °C after being left at −80 °C for 10 min. To further remove debris, the supernatant was applied for the first filtration (0.45 μm filter) and centrifugation (at 10,000×*g* for 10 min at 4 °C), and the second filtration (0.22 μm filter) and centrifugation. Each sample solution from the brain was subjected to HPLC.

Concentrations of BRC in the serum and brain samples were determined by HPLC on a Capcell Pak C18 column (Shiseido) with 50% acetonitrile in 10 mM phosphate buffer (pH 7.0).

Observation of gross phenotypes in mice

Mice were weighted daily and assessed for gross behavior every week from 12 weeks of age until death. In particular, hind limb movement and rearing behavior of each animal were monitored weekly from 12 weeks of age until the end stage. The days from the disease onset to the endpoint were counted individually as the survival interval.

Assessment of motor function

We assessed motor performance and coordination, and balance in the mice by the balance beam, vertical pole, and footprint tests. To determine the age that mice advanced to Grade1 (unable to stay on bar), the balance beam test was performed every day after the onset (Grade 3). The vertical pole (500 mm long and 9 mm in diameter) test was performed once a week until the mouse was incapable of the task. Each mouse was given five trials of the vertical pole test, and the highest vertical ascending distance was scored. The footprint trial was conducted at 16, 21, and 22 weeks of age. Front and hind paws were colored with blue and red inks, respectively. Stride length was defined as the distance between prints made by hind limbs. The test was performed until at least four clear continuous prints of both right and left hind limbs were obtained, and each distance between steps of both hind limbs was measured. The mice that accidentally died or showed unmeasurable scores on vertical pole test and/or stride length at a late symptomatic stage (21–22 weeks of age) were omitted from the statistical analyses.

Histopathological analysis

At a late symptomatic stage (21–22 weeks of age), mice were anesthetized with halothane (4%) in a mixture of N_2O/O_2 (70:30). Under anesthesia, mice were transcardially perfused with physiological saline containing 10% heparin, followed by 4% paraformaldehyde in 0.1 M phosphate buffer (pH 7.2). The spinal cord was removed and post-fixed with the same fixative for 48 h at 4 °C. Lumbar segment (3–4 mm in length) was embedded in paraffin. Serial transverse sections (6 μm thickness) of the lumbar segment (L4–L5) were sliced and stained with hematoxylin and eosin (H&E) for histopathological evaluation.

Immunohistochemical analysis

Immunohistochemical analyses with anti-ChAT, anti-Iba-1, anti-GFAP, anti-TNF-α, and anti-8-OHdG antibodies were performed. For immunostaining with anti-ChAT antibody, the deparaffinized sections from late symptomatic mice were pre-treated by autoclaving at 121 °C for 5 min in Histofine antigen retrieval solution (pH 9.0) (Nichirei). For immunostaining with anti-Iba-1 antibody, the deparaffinized sections from late symptomatic mice were pre-treated by autoclaving at 121 °C for 5 min in 10 mM citrate buffer (pH 6.0). For immunostaining with anti-GFAP antibody, the deparaffinized sections were used without any pretreatments. The sections were incubated with 0.3% H_2O_2 in methanol for 30 min and then with phosphate-buffered saline (PBS) (pH 7.2) containing 0.3% Triton X-100 for 30 min. After the treatment with PBS containing 5% normal goat serum (NGS) (Vector Laboratories)/0.05% Triton X-100 or 5% normal rabbit serum (NRS) (Vector Laboratories)/0.05% Triton X-100 for 1 h at room temperature, the sections were incubated with anti-GFAP antibody solution or with either anti-Iba-1 or anti-ChAT antibody in PBS containing 1.5% NRS/0.05% Triton X-100 overnight at 4 °C. The sections were then incubated with Histofine simple stain mouse Max-Po (R) (Nichirei) or with Histofine simple stain mouse Max-po (G) (Nichirei) for 1 h at room temperature. The sections were visualized using 0.05% 3,3-diaminobenzidine tetrahydrochloride (DAB) (Wako) and 0.015% H_2O_2 in 50 mM Tris–HCl (pH 7.5) buffer, and the DAB reaction products were observed under a light microscope (Biorevo BZ-9000, Keyence).

For immunostaining with anti-TNF-α antibody, the deparaffinized sections from late symptomatic mice were pre-treated by autoclaving at 121 °C for 5 min in 10 mM citrate buffer (pH 6.0). The sections were incubated with 0.3% H_2O_2 in methanol for 30 min. After the treatment with PBS containing 5% NRS/0.05% Triton X-100 for 1 h at room temperature, the sections were incubated with anti-TNF-α antibody in PBS containing 1.5% NRS/0.05% Triton X-100 overnight at 4 °C. The sections were then incubated with Histofine simple stain mouse Max-Po (G) for 1 h at room temperature. The sections were visualized using 0.05% DAB and 0.015% H_2O_2 in 50 mM Tris–HCl (pH 7.5) buffer, and the DAB reaction products were observed under a light microscope (Biorevo BZ-9000, Keyence).

For double immunostaining, the deparaffinized sections from late symptomatic mice were pre-treated by autoclaving at 121 °C for

10 min in 10 mM citrate buffer (pH 6.0). After the treatment with PBS containing 5%NGS/0.05% Triton X-100, the sections were incubated with anti-8-OHdG and anti-MAP2 or anti-GFAP antibodies in PBS containing 1.5% NGS/0.05% Triton X-100 overnight at 4 °C. The sections were then incubated with CF™555 Goat anti-mouse IgG (H + L) (dilution in 1:200) (Biotium) and CF™488 Goat anti-rabbit IgG (H + L) (dilution in 1:200) (Biotium) in PBS containing 1.5% NGS/0.05% Triton X-100 for 1 h at room temperature, coverslipped using glycerol/PBS containing anti-bleaching agent, and observed under a light microscope (Biorevo BZ-9000, Keyence).

Quantitative analysis of the number of motor neurons in L4–L5 lumbar segment from mice at a late symptomatic stage was conducted. Sections (6 μm thickness) were immunostained with anti-ChAT (see above), a marker of motor neurons, and observed under a light microscope (Biorevo BZ-9000, Keyence). A total of 17 representative images of every tenth serial section throughout L4–L5 segment were analyzed. A size of neuron (cross-sectional area of each soma) was also determined by utilizing BZ-II Analyzer (Keyence). ChAT-positive neurons were counted as those fulfilling the following two criteria; neurons located within ventral half of the gray matter of the spinal cord (see Fig. 3D) and neurons whose the cross-sectional area was >200 μm^2.

In vitro cell viability assay

The human dopaminergic neuroblastoma cell line SH-SY5Y was obtained from ATCC (CRL-2266). Cells were maintained at 37 °C in a humid 5% CO_2–95% air in Dulbecco's modified Eagle's medium (DMEM) supplemented with 10% fetal bovine serum (FBS), 100 U/ml penicillin and 100 μg/ml streptomycin. Culture medium was changed twice a week during cell growth. Cells at a density of 7.5×10^3 cells/well in 96-well culture plate were differentiated by the incubation with 5 μM *all-trans*-retinoic acid (RA) for 5 days, and used for the following cell viability assays. To investigate the effects of dopamine receptor antagonists on the BRC-associated protection against menadione-induced cell death, cells were preincubated for 30 min with either SCH23390 (SCH; 20 μM), Sulpiride (Sul; 20 μM), or Raclopride (Rac; 20 μM), and then treated with 40 μM BRC. After 24 h, medium was changed, and cells were exposed to 40 μM menadione for 4 h. For the analysis of the BRC's neuroprotective effect against various cytotoxins, cells were treated with 40 μM BRC for 24 h. After medium change, cells were exposed to 40 μM menadione (free radical generating compound) for 4 h, 13 μM α-naphtoquinone (free radical generating compound) for 4 h, 800 μM cisplatin (DNA-damaging reagent) for 30 h, 25 μM staurosporine (kinase inhibitor) for 6 h, 0.5 μM okadaic acid (phosphatase inhibitor) for 6 h, or 250 μM etoposide (topoisomerase II inhibitor) for 30 h. For cell viability, cells were treated with 0–50 μM BRC for 20 h. After medium change, cells were exposed to 40 μM menadione for 4 h. Cells treated with DMSO were used as controls. Cell viability was measured by the Alamar blue assay according to the manufacturer's protocol (Invitrogen).

Western blot analysis

Mice were anesthetized at a late symptomatic stage (21–22 weeks of age) with halothane (4%) in a mixture of N_2O/O_2 (70:30) and transcardially perfused with physiological saline containing 10% heparin, followed by excision of the lumbar spinal cord. We homogenized tissues in lysis buffer [50 mM Tris–HCl (pH 7.5), 150 mM NaCl, 1% NP-40, Complete Protease Inhibitor Cocktail (Roche), protein phosphatase inihibitor cocktail (Nacalai tesque)]. After centrifugation at 22,000 × *g* for 30 min at 4 °C, we collected the resultant supernatant as a NP-40 soluble fraction. We determined protein concentration by the Pierce 660 nm Protein Assay system (Thermo Fisher Scientific). Protein samples (5–10 μg) were electrophoretically separated on a 5–20% SDS-polyacrylamide gel (Wako), and transferred onto polyvinylidene difluoride (PVDF) membrane (Bio-Rad Laboratories).

Differentiated SH-SY5Y cells (3×10^5 cells) treated with BRC were washed twice with ice-cold PBS and were incubated in 1 ml of ice-cold 10% trichloroacetic acid solution for 30 min, and then were centrifuged at 22,000 × *g* for 15 min at 4 °C. The pellets were lysed with 80 μl of 9 M urea containing 2% Triton X-100 and 1% dithiothreitol. After the addition of 20 μl of 10% lithium dodecyl sulfate and 2 μl of 2 M Tris base, lysates were sonicated for reduced viscosity. Nuclear extracts were prepared from undifferentiated SH-SY5Y cells (3×10^5 cells) treated with BRC using a nuclear extraction kit (Active Motif) according to the manufacturer's protocol. Protein concentration was quantified by Pierce 660 nm Protein Assay kit using bovine serum albumin as a standard. Protein samples (5–10 μg) were electrophoretically separated on a 5–20% SDS-polyacrylamide gel (ATTO or Wako) and transferred onto PVDF membrane.

Membrane was blocked with Blocking One (Nacalai tesque) for 1 h at room temperature and then incubated with the primary antibody in Can Get signal solution 1 (Toyobo) overnight at 4 °C. After washing with TBST buffer [50 mM Tris–HCl (pH 7.4), 150 mM NaCl, 0.1% (w/v) Tween-20], membranes were incubated with the peroxidase-conjugated secondary antibody in Can Get signal solution 2 (Toyobo) for 1 h at room temperature. After washing with TBST, signals were visualized by Immobilon Western HRP substrate (Millipore) and Amersham Hyperfilm™ ECL (GE Healthcare).

Measurement of TNF-α in culture medium

Primary astrocyte cultures were established from the cerebral cortex of E19 mouse embryos. In brief, the cerebral cortex was isolated, placed into 5 ml of ice-cold PBS devoid of calcium and magnesium ion [PBS(−)], and dissected into small pieces. After removing PBS(−) by aspiration, 3 ml of 0.25% trypsin–0.01% DNase I was added and incubated for 15 min at 37 °C, and then 3 ml of horse serum was added to terminate trypsin–DNase I reaction. The tissue mixtures were centrifuged at 50 × *g* for 3 min, and the resulting tissue pellets were suspended in 5 ml of DMEM supplemented with 10% FBS by pipeting. Primary astrocytes were then seeded on 100-mm dish (BD Falcon), and grown for 4 days in DMEM supplemented with 10% FBS at 37 °C in a humid 5% CO_2–95% air.

Primary astrocytes (1×10^4 cells/cm^2) were exposed to LPS (1 μg/ml) for 24 h after pre-treatment with 20 μM BRC or DMSO (vehicle control) for 24 h. The concentration of TNF-α in the culture medium was determined using Murine TNF-α ELISA Development Kit (PeproTech) according to the manufacturer's instructions.

Detection of protein carbonyl groups

Mice were anesthetized at a late symptomatic stage (21–22 weeks of age) with halothane (4%) in a mixture of N_2O/O_2 (70:30) and transcardially perfused with physiological saline containing 10% heparin, followed by excision of the soleus muscle. Oxidatively modified proteins in the soleus muscle (0.7 μg of protein samples) were detected by immunoblotting using the OxyBlot™ Protein Oxidation Detection Kit (Millipore) according to the manufacturer's instructions. The levels of protein carbonyl groups were quantified by densitometric analysis.

Glutathione measurement

SH-SY5Y cells (7.5×10^3 cells/well) were plated in a 96-well plate, and then were differentiated by incubation with 5 μM *all-trans*-RA for 5 days. Differentiated SH-SY5Y cells were treated with various concentrations of BRC (in a range between 10 and 50 μM) or vehicle control (DMSO). After 20 h, the total cellular glutathione was

measured using the GSH-Glo™ Glutathione Assay kit (Promega) according to the manufacturer's instructions.

Reverse transcriptase-polymerase chain reaction (RT-PCR)

Total RNA was extracted from cells using the TRIzol reagent (Invitrogen). Isolated total RNA was purified using the SV Total RNA Isolation System (Promega) according to the manufacturer's protocol. RT-PCR was performed with QIAGEN OneStep RT-PCR kit (QIAGEN). The housekeeping gene of human peptidylprolyl isomerase A (*PPIA*) was used as an internal control. PCR primers specific to each gene and its target size are as follows: Nrf2, 5′-CGGTATGCAACAGGACATTG-3′, and 5′-ACTGGTTGGGGTCTTCTGTG-3′ (263 bp); HO-1, 5′-ACATCTATGTGGCCCTGGAG-3′, and 5′-TGTTGGGGAAGGTGAAGAAG-3′ (348 bp); ATF3, 5′-CTCCTGGGTCACTGGTGTTT-3′, and 5′-AGGCACTCCGTCTTCTCCTT-3′ (268 bp); GCLM, 5′-TTTGGTCAGGGAGTTTCCAG-3′, and 5′-TGGTTTTACCTGTGCCCACT-3′ (367 bp); NQO1, 5′-CATTCTGAAAGGCTGGTTTGA-3′, and 5′-TTTCTTCCATCCTTCCAGGAT-3′ (298 bp); PPIA, 5′-GACCCAACACAAATGGTTCC-3′, and 5′-TCGAGTTGTCCACAGTCAGC-3′ (184 bp). Amplified products were electrophoretically separated on a 2.0% agarose gel, stained with ethidium bromide, and photographed under ultraviolet light.

Statistical analysis

Data in this study were expressed as mean ± SD or mean ± SEM. Statistical significance was evaluated by ANOVA (analysis of variance) followed by Scheffe's *post hoc* test for multiple comparisons between groups and by unpaired Student's *t*-test for comparisons between the data of two groups (Excel statistics 2008). Survival data were compared using Kaplan–Meier survival analysis with log-rank test (SPSS 17.0 software). We considered p-values <0.05 to be statistically significant.

Results

Concentrations of BRC in the brain and serum

To confirm the blood–brain barrier penetration of BRC in mice, we determined the area under the curve (AUC) of BRC in the brain and serum after 10 mg/kg BRC intraperitoneal injection. The AUC of BRC in the brain and serum were 47.4 ± 13.8 ng·h/g (n = 4) and 348.9 ± 170.6 ng·h/ml (n = 4), respectively.

BRC abates disease progression in ALS(SOD1^{H46R}) mice

To evaluate the effect of BRC on disease symptoms, we conducted a daily post-onset administration of BRC [0 mg/kg (vehicle), 1 mg/kg or 10 mg/kg body weight] in combination with/without riluzole, or riluzole alone (vehicle/riluzole) to ALS(SOD1^{H46R}) mice. The average day of disease onset was 125.7 ± 2.9 days (n = 162). At 155 days of age, a majority of the vehicle-treated mice showed a complete paralysis of hind limbs, and thus never showed the feet-clasping phenotype upon the tail suspension and a rearing behavior (Fig. 1A, a and c). In contrast, the BRC-treated mice (10 mg/kg body weight) at the same age still showed a feet-clasping phenotype and rearing activity (Fig. 1A, b and d). Despite the significant effects, BRC did not affect the weight in this study (Fig. 1B).

BRC sustains motor performance in ALS(SOD1^{H46R}) mice

To assess whether BRC preserves motor functions in ALS(SOD1^{H46R}) mice, we conducted the balance beam test, the vertical pole test and footprint analysis. The balance beam test revealed that BRC treatment prolonged the interval from onset to Grade 1 (unable to stay on the bar). The intervals were significantly extended in 1 mg/kg and 10 mg/kg BRC-treated groups (23.2 ± 1.0 days and 24.5 ± 0.9 days, respectively) compared with vehicle-treated controls (20.2 ± 1.1 days) (Fig. 1C). The vertical pole test demonstrated that there was no observable difference in the ability to perform vertical pole climbing between BRC and vehicle-treated groups at a late pre-symptomatic stage (16–17 weeks) (Fig. 1D). However, at a symptomatic stage (21 weeks), 10 mg/kg BRC-treated group showed significant preservation when compared with vehicle control (Fig. 1D).

On the footprint analysis, all mice at 16 weeks of age, pre-symptomatic stage, showed almost normal ambulation (Fig. 1E). At a late symptomatic stage (21–22 weeks of age), vehicle, mice in the control group, showed an abnormal gait with reduced foot stride length and dragging of the legs, whereas age-matched mouse treated with 10 mg/kg BRC showed a short but still steady gait (Figs. 1E and F). These results demonstrate that the BRC treatment effectively sustains the motor function in ALS(SOD1^{H46R}) mice.

No beneficial effect of the treatment with riluzole on motor function

Currently, riluzole is the only FDA-approved drug for the ALS treatment, although it has only a modest impact (Bensimon et al., 1994; Miller et al., 2007). Next, we investigated whether BRC in combination with riluzole would further ameliorate symptoms of ALS (SOD1^{H46R}) mice. The feet-clasping phenotype and rearing behavior was observed in ALS(SOD1^{H46R}) mice treated with BRC/riluzole at 159 days of age (Supplmentary Fig. 1A, b and d), while mice treated with vehicle/riluzole (158 days of age) showed a complete paralysis of hind limbs at the same age (Supplementary Fig. 1A, a and c). No synergestic effects of BRC/riluzole including the weight gain or loss were observed (Fig. 1B and Supplementary Fig. 1B).

On the balance beam test and the footprint analysis, ALS (SOD1^{H46R}) mice treated with BRC/riluzole showed sustained motor performance compared to ALS(SOD1^{H46R}) mice treated with vehicle/riluzole (Supplementary. Figs. 1C, D and E). However, BRC in combination with riluzole treatment was not more effective than BRC treatment alone (Figs. 1C, E and F). These results indicate that there is no synergistic or additive therapeutic effect of riluzole on motor function.

BRC treatment prolongs a post-onset survival interval

We then evaluated the effect of BRC on disease progression in ALS (SOD1^{H46R}) mice using Kaplan–Meier survival analysis. The survival intervals after onset in BRC-treated animals at a dose of 1 mg/kg (39.0 ± 7.6 days) and 10 mg/kg (39.4 ± 7.1 days) were extended in comparison with those in vehicle group (35.2 ± 6.7 days) (Fig. 2).

Further, ALS(SOD1^{H46R}) mice treated with BRC/riluzole showed prolonged post-onset life span (38.8 ± 5.3 days) in comparison with ALS(SOD1^{H46R}) mice treated with vehicle/riluzole (35.4 ± 9.5 days) (Supplementary Fig. 1F).

These results indicate that BRC, but not riluzole, alleviates disease progression in ALS(SOD1^{H46R}) mice.

BRC treatment does not affect the SOD1 expression

To ensure that the administration of BRC did not alter the expression of the human *SOD1* transgene in ALS(SOD1^{H46R}) mice, we examined the levels of the SOD1 protein in the lumbar and sacral spinal cord by Western blot analysis (Supplementary Fig. 2). There were no significant differences in the NP-40 soluble mutant SOD1 levels between vehicle- and BRC-treated groups at a late symptomatic stage (21–22 weeks of age). These results indicate that BRC has no effect on mutant SOD1 expression, and that symptomatic amelioration observed in BRC-treated mice is not a consequence of SOD1 downregulation.

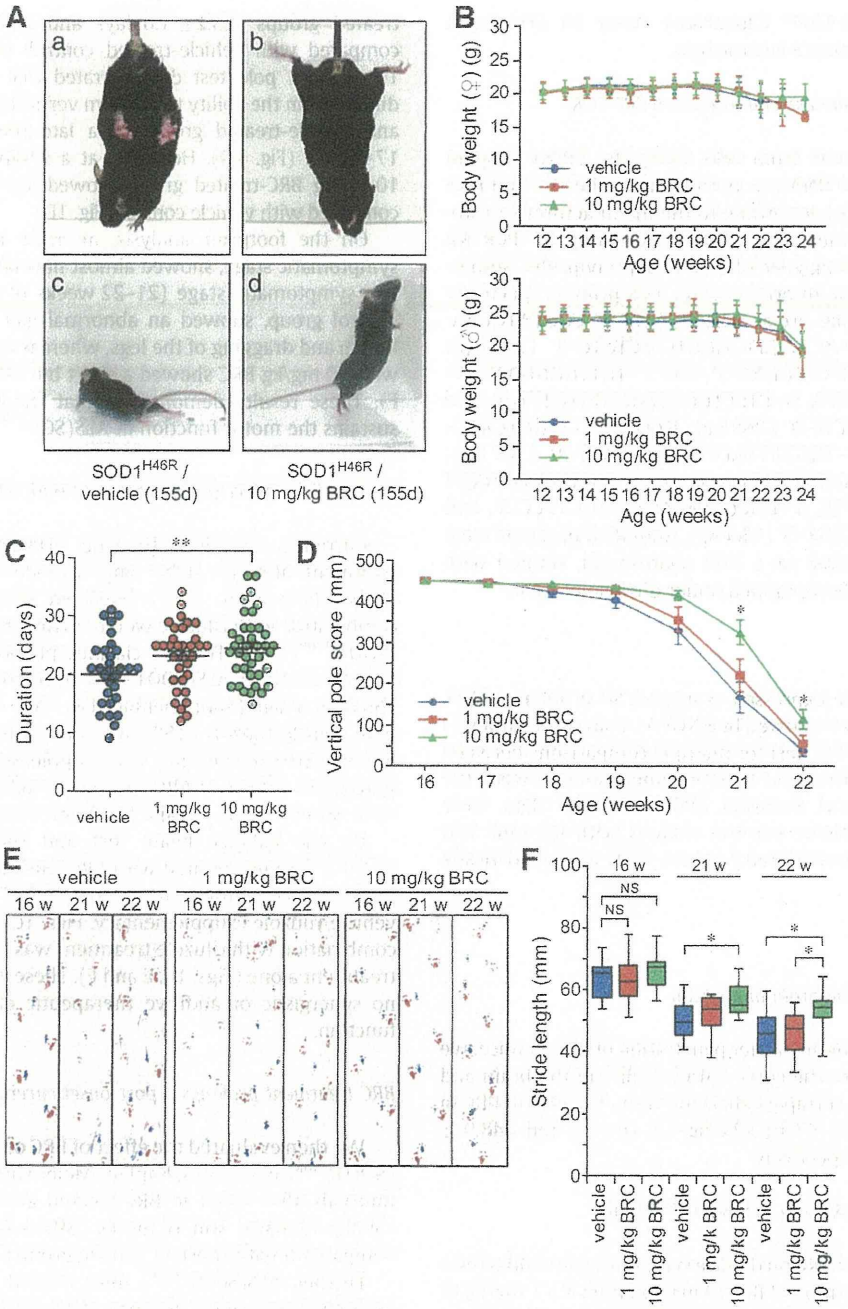

Fig. 1. Effect of the BRC treatment on the gross clinical symptoms in ALS(SOD1^{H46R}) mice. (A) Representative photographs of vehicle-treated (a and c) and BRC-treated (b and d) ALS (SOD1^{H46R}) mice showing a typical hind limb posture upon the tail suspension (a and b) and rearing behavior (c and d) at 155 days of age. (B) Changes in the body weight of female and male ALS(SOD1^{H46R}) mice in vehicle (female, n = 16 and male, n = 15) and BRC [1 mg/kg (female, n = 16 and male, n = 17) or 10 mg/kg (female, n = 19 and male, n = 19)]-treated groups between 12 and 24 weeks of age. Data are expressed as mean ± SD. (C) Scores of the balance beam test. Duration of date from the onset to the day at which each mouse was unable to stay on the bar was plotted. Data are expressed as mean ± SEM [vehicle (n = 31), 1 mg/kg BRC (n = 33) and 10 mg/kg BRC (n = 38)]. ** $p<0.01$ by one-way ANOVA with Scheffe's *post hoc* test. (D) Vertical pole scores of vehicle (n = 20), 1 mg/kg BRC (n = 23) and 10 mg/kg BRC (n = 23)-treated mice between 16 and 22 weeks of age. Data are expressed as mean ± SEM. * $p<0.05$ by one-way ANOVA with Scheffe's *post hoc* test when compared to the vehicle control. (E) Footprints of vehicle, 1 mg/kg BRC and 10 mg/kg BRC-treated mice at 16, 21 and 22 weeks of age. Blue, front paws; red, hind paws. (F) Box and whisker plots of stride length. Data indicate the average distance between the hind paw steps in vehicle (n = 14), 1 mg/kg BRC- (n = 18) and 10 mg/kg BRC (n = 18)-treated mice at 16, 21 and 22 weeks of age. The median is depicted as mid-horizontal lines, and upper and lower ends of boxes represent 75th and 25th percentiles, respectively. * $p<0.05$ by one-way ANOVA with Scheffe's *post hoc* test. NS, not significant.

BRC treatment reduces motor neuron loss in the spinal cord

To determine whether BRC protects motor neurons from the progressive dysfunction leading to the neuron loss, we counted ChAT-positive motor neurons in the spinal cord. At a late symptomatic stage (21–22 weeks of age), ALS(SOD1^{H46R}) mice treated with vehicle showed a massive loss of ChAT-positive motor neurons (Fig. 3B) compared with non-transgenic (non-Tg) littermates (Fig. 3A). Notably, ChAT-positive motor neurons of ALS(SOD1^{H46R}) mice treated with BRC were relatively spared (Fig. 3C).

To confirm this finding, we conducted a quantitative analysis of the number of ChAT-positive motor neurons whose soma sizes were larger than 200 μm^2 in the anterior horn located within ventral half of the gray matter of the spinal cord (Fig. 3D). At a late symptomatic

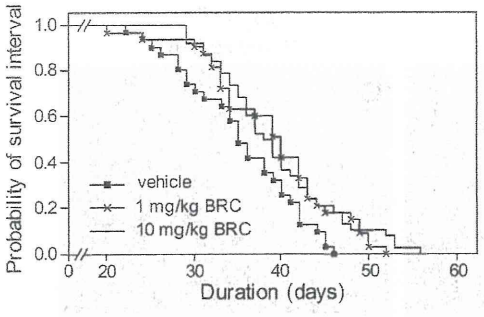

Fig. 2. Effect of the BRC treatment on the survival in ALS(SOD1^{H46R}) mice. The Kaplan–Meier curves demonstrate the probability of survival interval of vehicle control, 1 mg/kg BRC-treated and 10 mg/kg BRC-treated ALS(SOD1^{H46R}) mice. The average onset of ALS (SOD1^{H46R}) mice was 125.7 ± 2.9 days (n = 162). Survival intervals in BRC-treated groups at doses of 1 mg/kg (39.0 ± 7.6 days, n = 33) and 10 mg/kg (39.4 ± 7.1 days, n = 38) were significantly longer than that in vehicle group (35.2 ± 6.7 days, n = 31) ($p<0.05$ by log-rank test). These data are expressed as mean ± SD.

stage (21–22 weeks of age), vehicle-treated ALS(SOD1^{H46R}) mice (n = 4) showed a 36.4% loss of ChAT-positive motor neurons when compared with non-Tg littermates (n = 4) (Fig. 3E). By contrast, BRC-treated ALS(SOD1^{H46R}) mice (n = 4) showed a 23.3% loss of ChAT-positive motor neurons (Fig. 3E). Further, the BRC treatment preferentially preserved larger ChAT-positive motor neurons (>400 μm^2) in SOD1^{H46R} mice (Fig. 3F). These results indicate that BRC moderately protects motor neurons in the spinal cord from progressive degeneration in an ALS(SOD1^{H46R}) mouse model.

BRC treatment reduces reactive astrocytes

Astrogliosis and microglial activation are prominent histopathological hallmarks of the spinal cord in ALS patients and mutant SOD1-expressing mouse model of ALS (Hall et al., 1998; Kawamata et al., 1992; Schiffer et al., 1996). To assess whether the BRC treatment affects the glial cell activation at sites of motor neuron loss in ALS (SOD1^{H46R}) mice, we immunostained lumbar L4–L5 sections with anti-GFAP (for astrocytes) and anti-Iba-1 (for activated microglia) antibodies. At a late symptomatic stage (21–22 weeks of age), vehicle-treated ALS(SOD1^{H46R}) mice showed marked immunoreactivity both for GFAP and Iba-1 in the anterior horn of the lumbar spinal cord (Figs. 4E and H), normally the site of motor neurons loss (Fig. 4B), while the lumbar spinal cord of non-Tg siblings was almost devoid of immunoreactivity (Figs. 4D and G). BRC-treated ALS(SOD1^{H46R}) mice exhibited significantly less GFAP (Fig. 4F) and a slightly decreased Iba-1 (Fig. 4I) immunoreactivity in the anterior horn accompanied by the preservation of anterior horn cells (Fig. 4C) compared with vehicle-treated ALS(SOD1^{H46R}) mice (Fig. 4B). Further, Western blot analysis showed a marked decrease in the level of GFAP in BRC-treated ALS (SOD1^{H46R}) mice compared to those in vehicle-treated ALS (SOD1^{H46R}) mice (Figs. 5A and C), while the BRC treatment did not affect the level of the Iba-1 protein in ALS(SOD1^{H46R}) mice (Figs. 5B and D). These results indicate that the BRC treatment alleviates astrogliosis in the spinal cord of ALS(SOD1^{H46R}) mice.

BRC treatment decreases the levels of inflammatory factors

As reactive astrocytes intensify the production of inflammatory factors (Barbeito et al., 2004; Moisse and Strong, 2006), we next

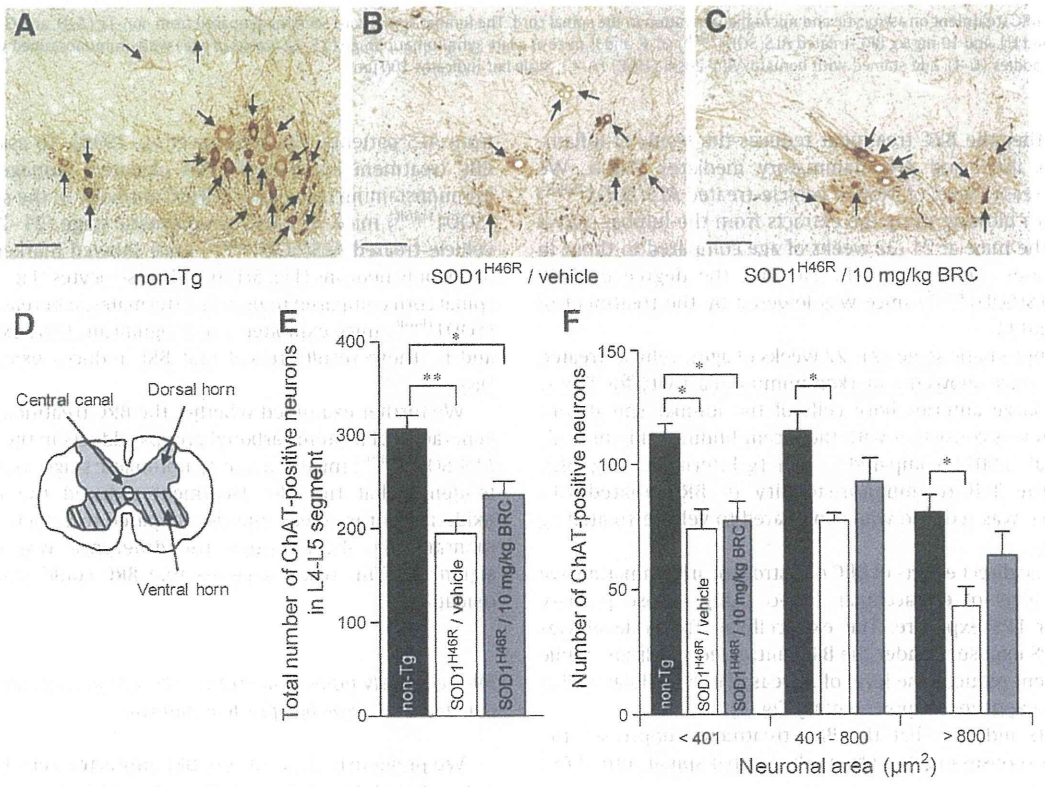

Fig. 3. Effect of the BRC treatment on motor neuron loss in the spinal cord. Representative images for immunohistochemical staining with anti-ChAT antibody in the anterior horn of the lumbar spinal cord (L4–L5) prepared from non-Tg (A), vehicle-treated ALS(SOD1^{H46R}) (B), and 10 mg/kg BRC-treated ALS(SOD1^{H46R}) (C) mice at a late symptomatic stage (21–22 weeks of age). Arrows indicate ChAT-positive motor neurons. Scale bar indicates 100 μm. The number of the neurons within the hatched region (D) of the cross-sectional L4–L5 segment in the lumbar spinal cord was counted. The total number (E) and the size distribution (F) of ChAT-positive neurons (>200 μm^2) within the ventral half of the gray matter (hatched region shown in D) in the L4–L5 lumbar spinal cord of non-Tg (n = 4), vehicle-treated ALS(SOD1^{H46R}) (n = 4), and 10 mg/kg BRC-treated ALS(SOD1^{H46R}) mice (n = 4). Data are expressed as mean ± SEM. ** $p<0.01$, * $p<0.05$ by one-way ANOVA with Scheffe's *post hoc* test.

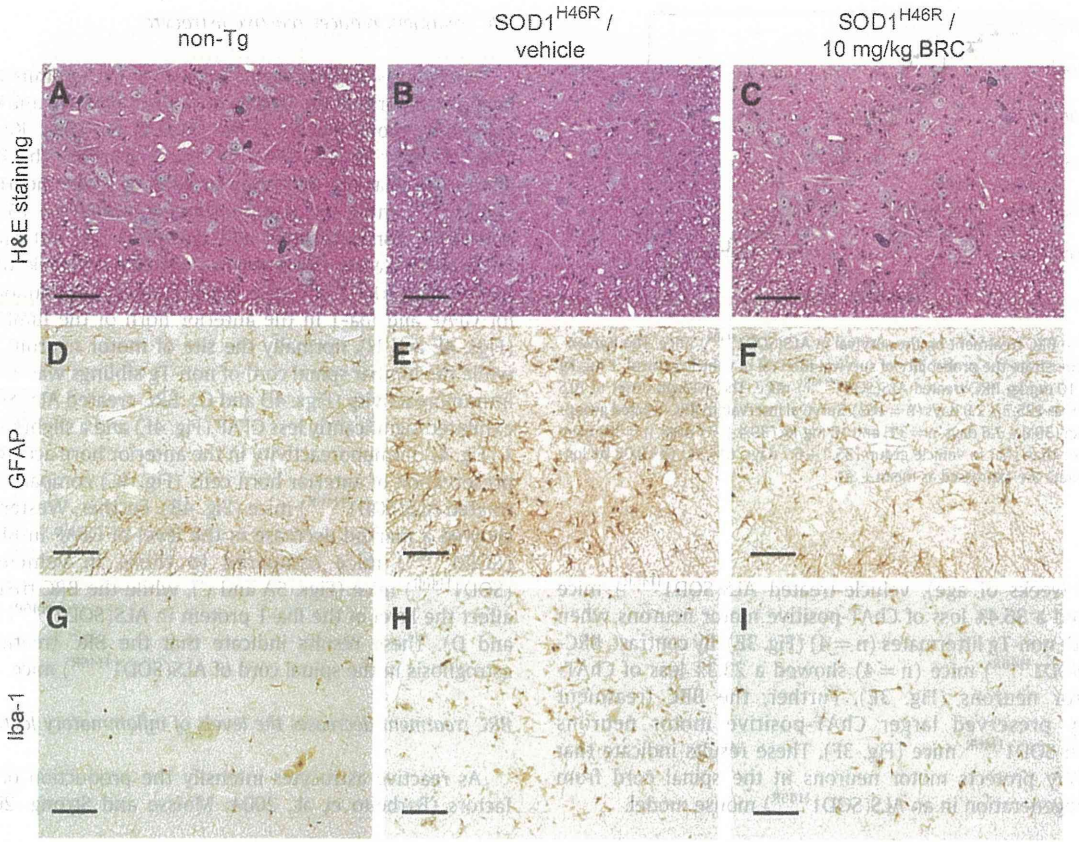

Fig. 4. Effect of the BRC treatment on astrocytic and microglial activation in the spinal cord. The lumbar spinal cord sections prepared from non-Tg (A, D, and G), vehicle-treated ALS ($SOD1^{H46R}$) (B, E, and H), and 10 mg/kg BRC-treated ALS($SOD1^{H46R}$) (C, F, and I) mice at a late symptomatic stage (21–22 weeks of age) were immunostained with anti-GFAP (D–F) and anti-Iba-1 antibodies (G–I), and stained with hematoxylin–eosin (H&E) (A–C). Scale bar indicates 100 μm.

examined whether the BRC treatment reduces the levels of inflammatory marker iNOS and proinflammatory mediator TNF-α. We detected an increased level of iNOS in vehicle-treated ALS($SOD1^{H46R}$) mice by Western blotting using the extracts from the lumbar–sacral spinal cord of the mice at 21–22 weeks of age compared to those in non-Tg littermates (Figs. 5E and F). Notably, the degree of iNOS induction in ALS($SOD1^{H46R}$) mice was lowered by the treatment of BRC (Figs. 5E and F).

At a late symptomatic stage (21–22 weeks of age), vehicle-treated ALS($SOD1^{H46R}$) mice showed a marked immunoreactivity for TNF-α particularly in large anterior horn cells of the lumbar spinal cord (Fig. 5G), which was consistent with the recent findings (Bigini et al., 2008; Petri et al., 2007), compared to non-Tg littermates (Fig. 5G). Importantly, the TNF-α imuunoreactivity in BRC-treated ALS ($SOD1^{H46R}$) mice was reduced when compared to vehicle-treated Tg animals (Fig. 5G).

To confirm the direct effects of BRC on astrocytic inflammation, we measured the level of extracellular TNF-α using mouse primary astrocytes after LPS exposure. The extracellular TNF-α level was increased by LPS exposure under the BRC-untreated condition, while the BRC treatment reduced the level of increased extracellular TNF-α induced by LPS exposure (Supplementary Fig. 3).

These results indicate that the BRC treatment suppresses the inflammatory responses in astrocytes in the lumbar spinal cord of ALS ($SOD1^{H46R}$) mice.

BRC treatment reduces oxidative damage in ALS($SOD1^{H46R}$) mice

Cellular constituents attacked by ROS include DNA, proteins, and lipids. Oxidative damage to DNA has been found in the spinal cord from ALS patients (Fitzmaurice et al., 1996). To assess whether the BRC treatment suppressed DNA oxidative damage, we performed immunostaining using anti-8OHdG antibody in the spinal cord of ALS ($SOD1^{H46R}$) mice. At a late symptomatic stage (21–22 weeks of age), vehicle-treated ALS($SOD1^{H46R}$) mice showed marked DNA oxidation in not only neurons (Fig. 5H) but also astrocytes (Fig. 5I) of the lumbar spinal cord compared to non-Tg littermates, whereas BRC-treated ALS ($SOD1^{H46R}$) mice exhibited a less significant DNA oxidation (Figs. 5H and I). These results reveal that BRC reduces oxidative damage to DNA.

We further examined whether the BRC treatment suppressed the generation of protein carbonyl groups adducts in the soleus muscle of ALS($SOD1^{H46R}$) mice at a late symptomatic stage. The result showed a tendency that the BRC treatment reduced the level of protein oxidation in the soleus muscle compared to vehicle control (Supplementary Fig. 4), although the difference was not statistically significant. This result suggests that BRC could also reduce protein oxidation.

BRC selectively protects neuronal cells against oxidative stress injury via dopamine receptor-independent pathway

We previously showed that BRC protected cells from menadione-induced oxidative stress (Okada et al., 2005). Here, we evaluated the effectiveness of BRC against various cytotoxins. Cell viability analysis revealed that BRC suppressed cell death induced by oxidative stressors, menadione and α-naphtoquinone (Supplementary Fig. 5A). However, it offered no protection against non-oxidative stressors, such as cisplatin, staurosporine, okadaic acid, and etoposide

(Supplementary Fig. 5A). These results indicate that BRC selectively protects cells from oxidative stress injury.

As BRC acts as a dopamine D2 receptor agonist (Radad et al., 2005), we tested whether the anti-oxidative cell death function of BRC is mediated via the activation of dopamine D2 receptor. Differentiated SH-SY5Y cells were treated with BRC in the presence or absence of dopamine receptor antagonists, and then exposed to the oxidative stress insult, menadione. Neither antagonist affected the protective effect of BRC against oxidative stress-induced cell death (Supplementary Fig. 5B). This result suggests that the neuroprotective effect of BRC in the ALS mice is independent of the dopamine D2 receptor activation.

BRC increases the level of antioxidant proteins

As GSH is an abundant antioxidant that scavenges reactive oxygen species, we investigated whether BRC affects the level of GSH in differentiated SH-SY5Y cells. As shown in Fig. 6A, we observed a BRC dose-dependent upregulation of GSH accompanied by increased cell viability.

Recent studies have demonstrated that the generation of GSH is associated with induction of ATF3 (Kim et al., 2010), and that BRC regulates the activation of Nrf2 and its downstream factor, NQO1, in PC12 cells (Lim et al., 2008). These results prompted us to investigate whether the BRC treatment induces mRNA expression of Nrf2-regulated genes including ATF3, HO-1, GCLM, and NQO1 in neuronal cell. As shown in Fig. 6B, the levels of both ATF3 and HO-1 mRNAs were increased in a BRC dose-dependent manner. However, the BRC treatment did not affect the expression levels of Nrf2, GCLM and NQO1 (Fig. 6B).

Consistent with increased mRNA expression, we detected increased level of ATF3 and HO-1 proteins (Fig. 6C). Notably, despite constant cellular levels of Nrf2 transcript, a greater fraction of Nrf2 was translocated into the nucleus upon the BRC treatment (Fig. 6D).

Collectively, these data suggest that BRC upregulates the levels of several anti-oxidative factors.

Discussion

There are a limited number of therapeutic strategies to effectively relieve symptoms and improve the quality of life for ALS patients. Although the molecular mechanism of the selective motor neuron death remains elusive, there is substantial evidence suggesting oxidative stress as one of the major factors underlying motor neuron loss (Barber et al., 2006). Our present study explored a novel therapeutic agent that could alleviate neural cell damage induced by oxidative stress in ALS.

Based on the anti-oxidative stress therapeutic strategy, we established NAIP-ELISA-based drug screening system to detect a transient upregulation of the endogenous NAIP level, and identified BRC as well as L-745,870 as NAIP-upregulating compounds (Okada et al., 2005). Indeed, we have shown that L-745, 870 alleviates disease progression and delays motor neuron loss accompanying with the suppression of microglial activation in the spinal cord of ALS ($SOD1^{H46R}$) mice (Tanaka et al., 2008). Importantly, the post-onset administration of L-745,870 also prolonged survival after onset (Tanaka et al., 2008).

On the other hand, BRC possesses free radical scavenging action and antioxidant property in *in vitro* and *in vivo* studies (Kitamura et al., 2003; Kondo et al., 1994; Lim et al., 2008; Ogawa et al., 1994; Yoshikawa et al., 1994). Further, BRC confers neuroprotection against ischemia-induced neuronal insults (Liu et al., 1995; O'Neill et al., 1998). In the present study, we sought to evaluate the neuroprotective effect of BRC in ALS($SOD1^{H46R}$) mice, and demonstrated that the post-onset administration of BRC significantly ameliorated clinical symptoms at late symptomatic stage (22 weeks of age) compared to vehicle control mice (Fig. 1A). Further, the BRC treatment prolonged 12% of the survival interval after onset in ALS($SOD1^{H46R}$) mice. Interestingly, BRC treatment mitigates motor neuron loss in the spinal cord accompanied by the suppression of reactive astrocytes and partly by the reduced level of microglial activation in ALS($SOD1^{H46R}$) mice.

Inflammatory response in ALS is characterized by the accumulation of large numbers of activated microglia and astrocytes (Glass et al., 2010; McGeer and McGeer, 2002). Accumulating evidence has indicated that perturbation of the crosstalk between astrocytes and neurons is associated with motor neuron degeneration (Di Giorgio et al., 2007; Nagai et al., 2007; Yamanaka et al., 2008), while microglia contributes to disease propagation (Boillee et al., 2006b). Previous studies have demonstrated that activated microglia induces the production of neurotoxic factors such as superoxide, nitric oxide and proinflammatory cytokines, while reactive astrocytes express inflammatory markers such as iNOS (Barbeito et al., 2004; Block et al., 2007; Moisse and Strong, 2006). Recent findings have also suggested the link between oxidative stress and inflammatory response in ALS (Barber and Shaw, 2010; Liu et al., 2009). In this study, we revealed that BRC treatment remarkably suppressed the activation of astrocytes in the spinal cord of ALS($SOD1^{H46R}$) mice. Moreover, BRC-treated ALS($SOD1^{H46R}$) mice showed a decreased level of iNOS and TNF-α. Consistent with *in vivo* data, BRC reduced TNF-α release by LPS treatment in mouse primary astrocytes, indicating a direct effect of BRC on astrocytes. In addition, BRC treatment reduced the level of DNA oxidation in neurons and astrocytes of the spinal cord in ALS ($SOD1^{H46R}$) mice. Although the detailed mechanism of the BRC effect on astrocytes remains elusive, our results strongly suggest that BRC attenuates astrogliosis and concomitantly reduces the levels of inflammatory factors and the oxidative damage in the spinal cord, thereby protecting from motor neuron loss.

Currently, the mechanisms by which BRC preserves motor neurons are still unclarified. A previous study has reported that BRC is associated with the induction of Nrf2-dependent antioxidant defense system, and that Nrf2-mediated cytoprotection of BRC is independent of dopamine D2 receptor (Lim et al., 2008). Consistent with these findings, our present study suggested that the cytoprotective effect of BRC against oxidative stress in SH-SY5Y neuronal cells was mainly mediated via a dopamine receptor-independent pathway, and that BRC increased the levels of Nrf2-regulated factors, such as HO-1. Besides, Nrf2 also mediates ATF3 induction that contributes to the cytoprotection of Nrf2 in astrocytes (Kim et al., 2010). ATF3 is required for the generation of GSH (Kim et al., 2010). In this study, we demonstrated for the first time that BRC treatment led to an increased level of ATF3 protein and to the GSH generation accompanying cytoprotection against oxidative stress in cultured cells. It has also been shown that depletion of GSH induces the release of proinflammatory factors (Lee et al., 2010). Our results showed decreased levels of not only iNOS and TNF-α, but also oxidative damage to DNA and protein in BRC-treated ALS($SOD1^{H46R}$) mice. Moreover, NAIP is known to selectively suppress oxidative stress-induced cell death (Liston et al., 1996). Taken together, it seems reasonable that BRC exerts its potency by the combined mechanism involving the enhanced NAIP-mediated cytoprotection, the activation of Nrf2 signaling cascades, and the upregulation of the ATF3-GSH axis in ALS($SOD1^{H46R}$) mice.

Preclinical animal studies are an essential step for the development of novel and effective therapeutic agents for the ALS treatment. However, the outcomes of drug efficacy tests using animal models were varied due to different methodological conditions such as the pre-symptomatic or the symptomatic administration of agent (Benatar, 2007; Turner and Talbot, 2008). A recently issued article outlining standard operating procedures for preclinical animal study for ALS/MND strongly recommends the use of post-onset administration of candidate agents to animal model because of the relevance to clinical settings (Ludolph et al., 2010). In the present study, we

conducted the BRC preclinical study in observance of these recommendations, and demonstrated an obvious neuroprotective activity of BRC in mutant SOD1 mouse model of ALS, proving the efficacy of BRC in the preclinical animal study. Thus, although the exact target of BRC on motor neuron protection in ALS(SOD1^{H46R}) mouse model remains unclear, BRC is a promising candidate as a therapeutic agent for the ALS treatment.

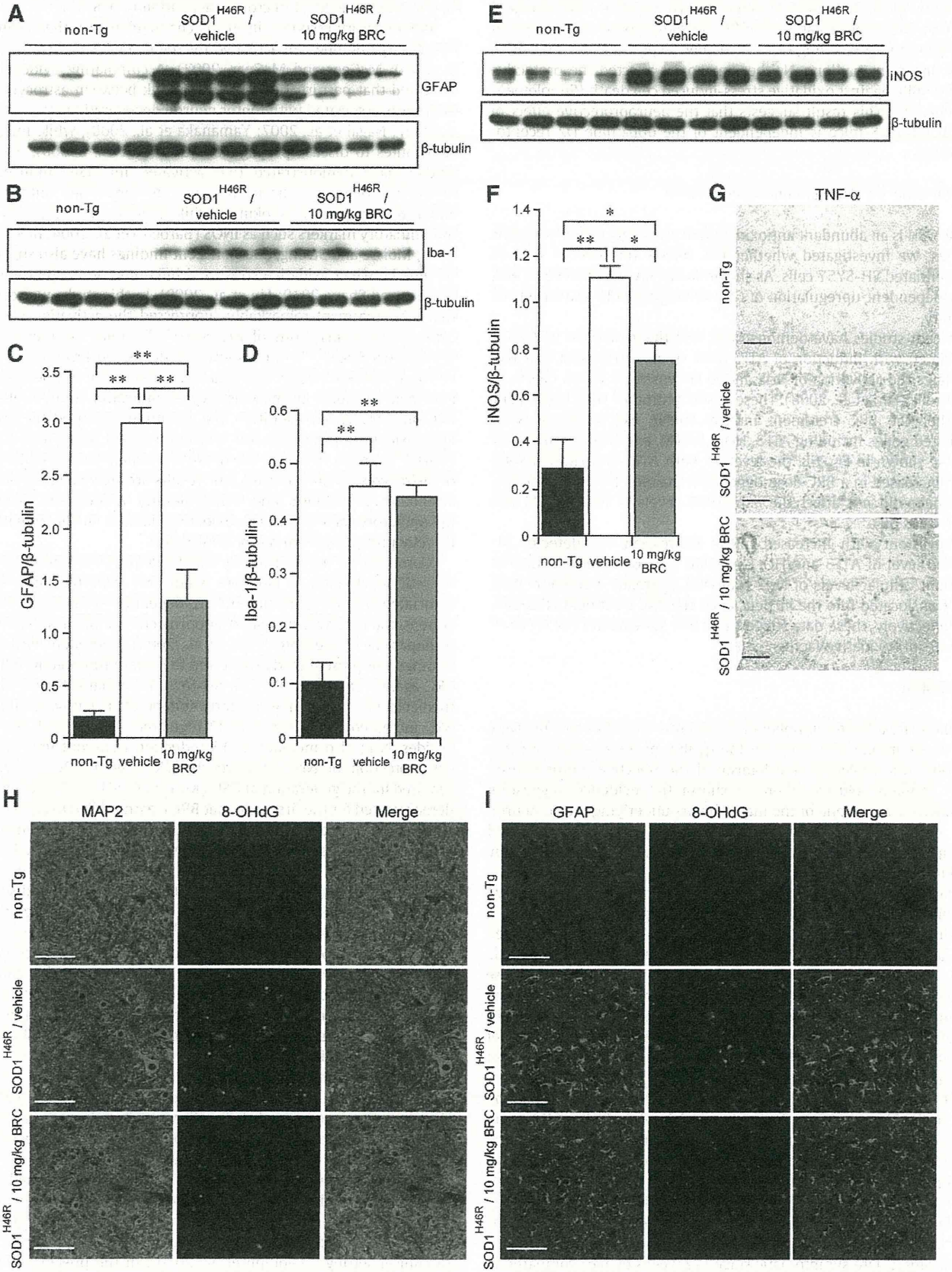

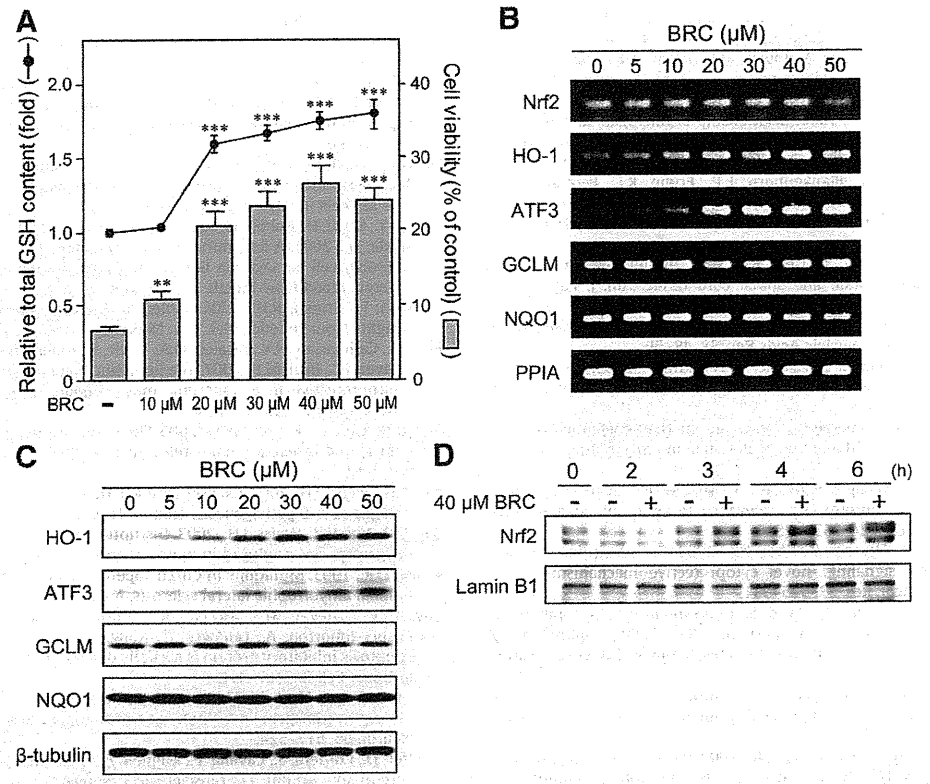

Fig. 6. Effect of BRC on the expression of anti-oxidative factors. (A) Differentiated SH-SY5Y cells were treated with the indicated concentrations of BRC for 20 h. Total intracellular GSH (black line) was measured by the levels of GSH and oxidized glutathione (GSSG), which were normalized to the number of cells. The values [mean ± SEM (n = 4)] relative to that of vehicle control are shown. For cell viability, after 20 h of treatment with the indicated concentration of BRC, cells were exposed to 40 μM menadione for 4 h. Cell viability (gray bars) was measured with the Alamar blue assay (Invitrogen). Data are expressed as mean ± SEM (n = 4). *** $p<0.001$, ** $p<0.01$ by one-way ANOVA with Scheffe's *post hoc* test compared with vehicle. (B) Differentiated SH-SY5Y cells were treated with the indicated concentrations of BRC for 6 h. The expression levels of Nrf2, HO-1, ATF3, GCLM, and NQO1 were assessed by RT-PCR. The housekeeping *PPIA* gene was used as an internal control. (C) Differentiated SH-SY5Y cells were treated with the indicated concentrations of BRC for 20 h. The proteins were analyzed by immunoblotting using anti-HO-1, anti-ATF3, anti-GCLM, anti-NQO1, or anti-β-tubulin antibody. (D) Effect of BRC on Nrf2-nuclear translocation. Undifferentiated SH-SY5Y cells were treated with 40 μM BRC at the indicated time. Nuclear fraction was analyzed by immunoblotting using anti-Nrf2 antibody. Lamin B1 was used as an internal control for nuclear fraction.

Supplementary materials related to this article can be found online at doi:10.1016/j.expneurol.2011.08.001.

Acknowledgments

This work was supported by the National Institute of Biomedical Innovation (NIBIO) (J.E.I.). We are grateful to Alex MacKenzie (CHEO) for inspired discussion and critical manuscript reading.

References

Barbeito, L.H., Pehar, M., Cassina, P., Vargas, M.R., Peluffo, H., Viera, L., Estevez, A.G., Beckman, J.S., 2004. A role for astrocytes in motor neuron loss in amyotrophic lateral sclerosis. Brain Res. Brain Res. Rev. 47, 263–274.

Barber, S.C., Mead, R.J., Shaw, P.J., 2006. Oxidative stress in ALS: a mechanism of neurodegeneration and a therapeutic target. Biochim. Biophys. Acta 1762, 1051–1067.

Barber, S.C., Shaw, P.J., 2010. Oxidative stress in ALS: key role in motor neuron injury and therapeutic target. Free Radic. Biol. Med. 48, 629–641.

Benatar, M., 2007. Lost in translation: treatment trials in the SOD1 mouse and in human ALS. Neurobiol. Dis. 26, 1–13.

Bensimon, G., Lacomblez, L., Meininger, V., 1994. A controlled trial of riluzole in amyotrophic lateral sclerosis. ALS/Riluzole Study Group. N. Engl. J. Med. 330, 585–591.

Bigini, P., Repici, M., Cantarella, G., Fumagalli, E., Barbera, S., Cagnotto, A., De Luigi, A., Tonelli, R., Bernardini, R., Borsello, T., Mennini, T., 2008. Recombinant human TNF-binding protein-1 (rhTBP-1) treatment delays both symptoms progression and motor neuron loss in the wobbler mouse. Neurobiol. Dis. 29, 465–476.

Block, M.L., Zecca, L., Hong, J.S., 2007. Microglia-mediated neurotoxicity: uncovering the molecular mechanisms. Nat. Rev. Neurosci. 8, 57–69.

Boillee, S., Vande Velde, C., Cleveland, D.W., 2006a. ALS: a disease of motor neurons and their nonneuronal neighbors. Neuron 52, 39–59.

Boillee, S., Yamanaka, K., Lobsiger, C.S., Copeland, N.G., Jenkins, N.A., Kassiotis, G., Kollias, G., Cleveland, D.W., 2006b. Onset and progression in inherited ALS determined by motor neurons and microglia. Science 312, 1389–1392.

Chang-Hong, R., Wada, M., Koyama, S., Kimura, H., Arawaka, S., Kawanami, T., Kurita, K., Kadoya, T., Aoki, M., Itoyama, Y., Kato, T., 2005. Neuroprotective effect of oxidized galectin-1 in a transgenic mouse model of amyotrophic lateral sclerosis. Exp. Neurol. 194, 203–211.

Cleveland, D.W., Rothstein, J.D., 2001. From Charcot to Lou Gehrig: deciphering selective motor neuron death in ALS. Nat. Rev. Neurosci. 2, 806–819.

Di Giorgio, F.P., Carrasco, M.A., Siao, M.C., Maniatis, T., Eggan, K., 2007. Non-cell autonomous effect of glia on motor neurons in an embryonic stem cell-based ALS model. Nat. Neurosci. 10, 608–614.

Fitzmaurice, P.S., Shaw, I.C., Kleiner, H.E., Miller, R.T., Monks, T.J., Lau, S.S., Mitchell, J.D., Lynch, P.G., 1996. Evidence for DNA damage in amyotrophic lateral sclerosis. Muscle Nerve 19, 797–798.

Fig. 5. Effect of the BRC treatment on the levels of GFAP, Iba-1, iNOS, and TNF-α, and on oxidative damage to DNA. The levels of the GFAP, Iba-1 and iNOS proteins in the lumbar spinal cord from ALS(SOD1^{H46R}) mice treated with vehicle or 10 mg/kg BRC at a late symptomatic stage (21–22 weeks of age) and from age-matched non-Tg littermates were analyzed. The NP-40 soluble fractions [5 μg (A and E) or 10 μg (B) proteins] were used for immunoblotting with anti-GFAP (A), anti-Iba-1 (B) or anti-iNOS antibody (E). Quantitative analyses of GFAP- (C), Iba-1- (D) and iNOS- (F) immunoreactive bands are shown. Data are expressed as mean ± SEM (n = 4). ** $p<0.01$, * $p<0.05$ by one-way ANOVA with Scheffe's *post hoc* test. (G) The ventral horn of the lumbar spinal cord from non-Tg, vehicle-treated ALS(SOD1^{H46R}), and 10 mg/kg BRC-treated ALS(SOD1^{H46R}) mice at a late symptomatic stage (21–22 weeks of age) were immunostained with anti-TNF-α. (H and I) Representative images of double immunostaining with anti-8-OHdG (red) and anti-MAP2 (for neurons) (green; H) and anti-GFAP (for astrocytes) (green; I) antibodies for the ventral horn of the lumbar spinal cord from non-Tg, vehicle-treated ALS(SOD1^{H46R}), and 10 mg/kg BRC-treated ALS (SOD1^{H46R}) mice at a late symptomatic stage (21–22 weeks of age). Scale bar indicates 100 μm.

Glass, C.K., Saijo, K., Winner, B., Marchetto, M.C., Gage, F.H., 2010. Mechanisms underlying inflammation in neurodegeneration. Cell 140, 918–934.
Gurney, M.E., Cutting, F.B., Zhai, P., Doble, A., Taylor, C.P., Andrus, P.K., Hall, E.D., 1996. Benefit of vitamin E, riluzole, and gabapentin in a transgenic model of familial amyotrophic lateral sclerosis. Ann. Neurol. 39, 147–157.
Hall, E.D., Oostveen, J.A., Gurney, M.E., 1998. Relationship of microglial and astrocytic activation to disease onset and progression in a transgenic model of familial ALS. Glia 23, 249–256.
Heiman-Patterson, T.D., Deitch, J.S., Blankenhorn, E.P., Erwin, K.L., Perreault, M.J., Alexander, B.K., Byers, N., Toman, I., Alexander, G.M., 2005. Background and gender effects on survival in the TgN(SOD1-G93A)1Gur mouse model of ALS. J. Neurol. Sci. 236, 1–7.
Kawamata, T., Akiyama, H., Yamada, T., McGeer, P.L., 1992. Immunologic reactions in amyotrophic lateral sclerosis brain and spinal cord tissue. Am. J. Pathol. 140, 691–707.
Kim, K.H., Jeong, J.Y., Surh, Y.J., Kim, K.W., 2010. Expression of stress-response ATF3 is mediated by Nrf2 in astrocytes. Nucleic Acids Res. 38, 48–59.
Kitamura, Y., Taniguchi, T., Shimohama, S., Akaike, A., Nomura, Y., 2003. Neuroprotective mechanisms of antiparkinsonian dopamine D2-receptor subfamily agonists. Neurochem. Res. 28, 1035–1040.
Kondo, T., Ito, T., Sugita, Y., 1994. Bromocriptine scavenges methamphetamine-induced hydroxyl radicals and attenuates dopamine depletion in mouse striatum. Ann. N. Y. Acad. Sci. 738, 222–229.
Lee, M., Cho, T., Jantaratnotai, N., Wang, Y.T., McGeer, E., McGeer, P.L., 2010. Depletion of GSH in glial cells induces neurotoxicity: relevance to aging and degenerative neurological diseases. FASEB J. 24, 2533–2545.
Lim, J.H., Kim, K.M., Kim, S.W., Hwang, O., Choi, H.J., 2008. Bromocriptine activates NQO1 via Nrf2-PI3K/Akt signaling: novel cytoprotective mechanism against oxidative damage. Pharmacol. Res. 57, 325–331.
Liston, P., Roy, N., Tamai, K., Lefebvre, C., Baird, S., Cherton-Horvat, G., Farahani, R., McLean, M., Ikeda, J.E., MacKenzie, A., Korneluk, R.G., 1996. Suppression of apoptosis in mammalian cells by NAIP and a related family of IAP genes. Nature 379, 349–353.
Liu, X.H., Kato, H., Chen, T., Kato, K., Itoyama, Y., 1995. Bromocriptine protects against delayed neuronal death of hippocampal neurons following cerebral ischemia in the gerbil. J. Neurol. Sci. 129, 9–14.
Liu, Y., Hao, W., Dawson, A., Liu, S., Fassbender, K., 2009. Expression of amyotrophic lateral sclerosis-linked SOD1 mutant increases the neurotoxic potential of microglia via TLR2. J. Biol. Chem. 284, 3691–3699.
Ludolph, A.C., Bendotti, C., Blaugrund, E., Chio, A., Greensmith, L., Loeffler, J.P., Mead, R., Niessen, H.G., Petri, S., Pradat, P.F., Robberecht, W., Ruegg, M., Schwalenstocker, B., Stiller, D., van den Berg, L., Vieira, F., von Horsten, S., 2010. Guidelines for preclinical animal research in ALS/MND: a consensus meeting. Amyotroph. Lateral Scler. 11, 38–45.
McGeer, P.L., McGeer, E.G., 2002. Inflammatory processes in amyotrophic lateral sclerosis. Muscle Nerve 26, 459–470.
Miller, R.G., Mitchell, J.D., Lyon, M., Moore, D.H., 2007. Riluzole for amyotrophic lateral sclerosis (ALS)/motor neuron disease (MND). Cochrane Database Syst. Rev. CD001447.
Moisse, K., Strong, M.J., 2006. Innate immunity in amyotrophic lateral sclerosis. Biochim. Biophys. Acta 1762, 1083–1093.
Nagai, M., Re, D.B., Nagata, T., Chalazonitis, A., Jessell, T.M., Wichterle, H., Przedborski, S., 2007. Astrocytes expressing ALS-linked mutated SOD1 release factors selectively toxic to motor neurons. Nat. Neurosci. 10, 615–622.
O'Neill, M.J., Hicks, C.A., Ward, M.A., Cardwell, G.P., Reymann, J.M., Allain, H., Bentue-Ferrer, D., 1998. Dopamine D2 receptor agonists protect against ischaemia-induced hippocampal neurodegeneration in global cerebral ischaemia. Eur. J. Pharmacol. 352, 37–46.
Ogawa, N., Tanaka, K., Asanuma, M., Kawai, M., Masumizu, T., Kohno, M., Mori, A., 1994. Bromocriptine protects mice against 6-hydroxydopamine and scavenges hydroxyl free radicals in vitro. Brain Res. 657, 207–213.
Okada, Y., Sakai, H., Kohiki, E., Suga, E., Yanagisawa, Y., Tanaka, K., Hadano, S., Osuga, H., Ikeda, J.E., 2005. A dopamine D4 receptor antagonist attenuates ischemia-induced neuronal cell damage via upregulation of neuronal apoptosis inhibitory protein. J. Cereb. Blood Flow Metab. 25, 794–806.
Pasinelli, P., Brown, R.H., 2006. Molecular biology of amyotrophic lateral sclerosis: insights from genetics. Nat. Rev. Neurosci. 7, 710–723.
Petri, S., Calingasan, N.Y., Alsaied, O.A., Wille, E., Kiaei, M., Friedman, J.E., Baranova, O., Chavez, J.C., Beal, M.F., 2007. The lipophilic metal chelators DP-109 and DP-460 are neuroprotective in a transgenic mouse model of amyotrophic lateral sclerosis. J. Neurochem. 102, 991–1000.
Radad, K., Gille, G., Rausch, W.D., 2005. Short review on dopamine agonists: insight into clinical and research studies relevant to Parkinson's disease. Pharmacol. Rep. 57, 701–712.
Rao, S.D., Weiss, J.H., 2004. Excitotoxic and oxidative cross-talk between motor neurons and glia in ALS pathogenesis. Trends Neurosci. 27, 17–23.
Rao, S.D., Yin, H.Z., Weiss, J.H., 2003. Disruption of glial glutamate transport by reactive oxygen species produced in motor neurons. J. Neurosci. 23, 2627–2633.
Rosen, D.R., 1993. Mutations in Cu/Zn superoxide dismutase gene are associated with familial amyotrophic lateral sclerosis. Nature 364, 362.
Roy, N., Mahadevan, M.S., McLean, M., Shutler, G., Yaraghi, Z., Farahani, R., Baird, S., Besner-Johnston, A., Lefebvre, C., Kang, X., et al., 1995. The gene for neuronal apoptosis inhibitory protein is partially deleted in individuals with spinal muscular atrophy. Cell 80, 167–178.
Sasaki, S., Nagai, M., Aoki, M., Komori, T., Itoyama, Y., Iwata, M., 2007. Motor neuron disease in transgenic mice with an H46R mutant SOD1 gene. J. Neuropathol. Exp. Neurol. 66, 517–524.
Schiffer, D., Cordera, S., Cavalla, P., Migheli, A., 1996. Reactive astrogliosis of the spinal cord in amyotrophic lateral sclerosis. J. Neurol. Sci. 139 (Suppl), 27–33.
Tanaka, K., Okada, Y., Kanno, T., Otomo, A., Yanagisawa, Y., Shouguchi-Miyata, J., Suga, E., Kohiki, E., Onoe, K., Osuga, H., Aoki, M., Hadano, S., Itoyama, Y., Ikeda, J.E., 2008. A dopamine receptor antagonist L-745,870 suppresses microglia activation in spinal cord and mitigates the progression in ALS model mice. Exp. Neurol. 211, 378–386.
Turner, B.J., Talbot, K., 2008. Transgenics, toxicity and therapeutics in rodent models of mutant SOD1-mediated familial ALS. Prog. Neurobiol. 85, 94–134.
Yamanaka, K., Chun, S.J., Boillee, S., Fujimori-Tonou, N., Yamashita, H., Gutmann, D.H., Takahashi, R., Misawa, H., Cleveland, D.W., 2008. Astrocytes as determinants of disease progression in inherited amyotrophic lateral sclerosis. Nat. Neurosci. 11, 251–253.
Yoshikawa, T., Minamiyama, Y., Naito, Y., Kondo, M., 1994. Antioxidant properties of bromocriptine, a dopamine agonist. J. Neurochem. 62, 1034–1038.

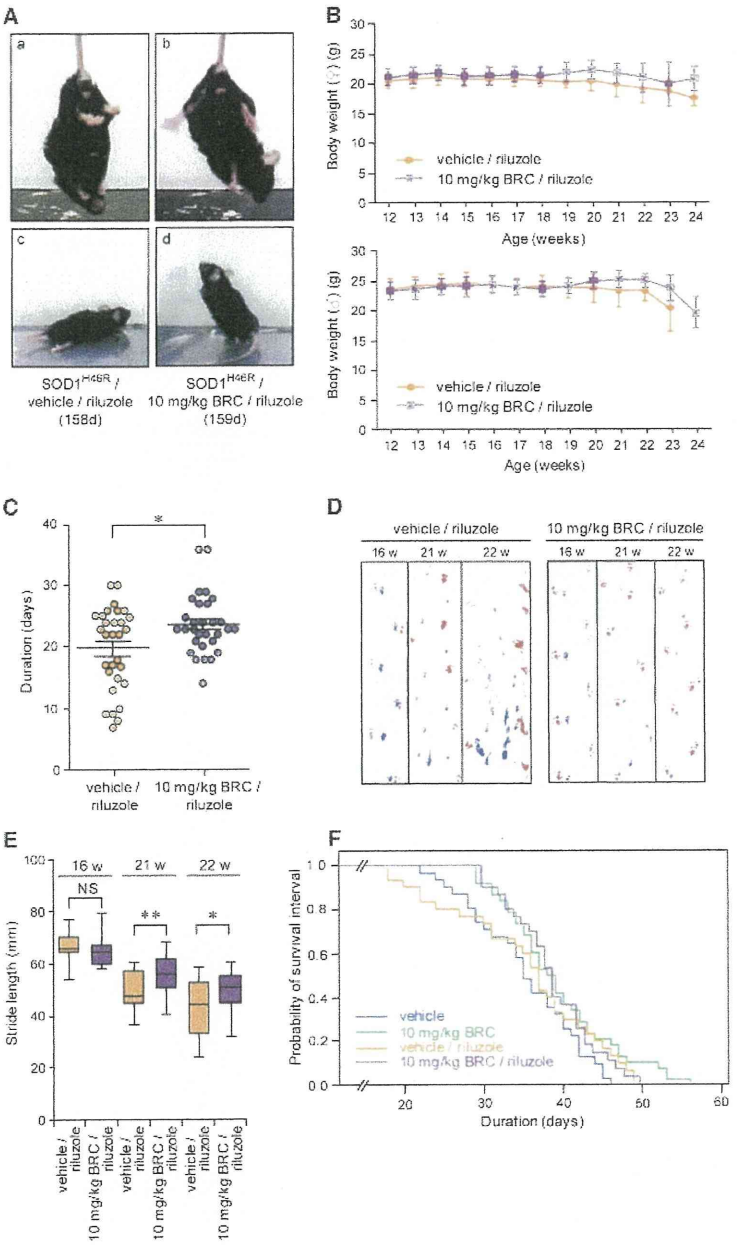

Supplementary Fig. 1. Effect of the combined BRC/riluzole treatment on the survival of ALS(SOD1^{H46R}) mice. (A) Representative photographs of vehicle/riluzole-treated (158 days of a 10 mg/kg BRC/riluzole-treated (159 days of age) (b and d) ALS(SOD1^{H46R}) mice showing a typical hind limb posture upon the tail suspension (a and b) and rearing behavior (c and d) body weight of female and male ALS(SOD1^{H46R}) mice in vehicle/riluzole (female, n = 15 and male, n = 15) and 10 mg/kg BRC/riluzole (female, n = 15 and male, n = 15)-treated group 24 weeks of age. Data are expressed as mean ± SD. (C) Scores of the balance beam test. Duration of date from the onset to the day at which each mouse was unable to stay on the Data are expressed as mean ± SEM [vehicle/riluzole (19.8 ± 1.2 days, n = 30) and 10 mg/kg BRC/riluzole (23.7 ± 0.9 days, n = 30)]. (D) Footprints of vehicle/riluzole- and 10 mg/kg B mice at 16, 21 and 22 weeks of age. Blue, front paws; red, hind paws. (E) Box and whisker plots of stride length. Data indicate the average distance between the hind paw steps in ve (n = 19) and 10 mg/kg BRC/riluzole (n = 23)-treated mice at 16, 21 and 22 weeks of age. The median is depicted as mid-horizontal lines, and upper and lower ends of boxes represer percentiles, respectively. ** $p < 0.01$, * $p < 0.05$ by Student's *t*-test compared with each corresponding control. (F) The Kaplan–Meier curves demonstrate the probability of survival int vehicle/riluzole-treated and 10 mg/kg BRC/riluzole-treated ALS(SOD1^{H46R}) mice. The average onset of ALS(SOD1^{H46R}) mice was 125.7 ± 2.9 days (n = 162). Survival intervals after th prolonged in 10 mg/kg BRC/riluzole-treated group (38.8 ± 5.3 days, n = 30) compared with vehicle/riluzole control group (35.4 ± 9.5 days, n = 30). These data are expressed as mean

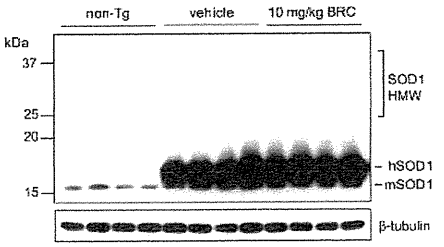

Supplementary Fig. 2. Effect of the BRC treatment on the mutant SOD1 level. The expression levels of the SOD1 protein in the lumbar spinal cord from ALS(SOD1^{H46R}) mice treated · 10 mg/kg BRC at a late symptomatic stage (21–22 weeks of age) (n = 4) and from age-matched non-Tg littermates (n = 4) were analyzed. The NP-40 soluble fractions (5 μg proteins) immunoblotting with anti-SOD1 antibody. hSOD1 and mSOD1 represent the mutated (H46R) human SOD1 protein and endogenous mouse SOD1 protein, respectively. β-tubulin was control.

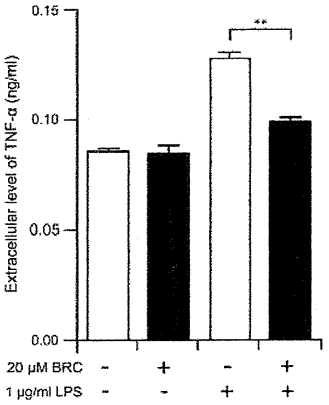

Supplementary Fig. 3. The level of TNF-α in BRC-treated astrocytes. Mouse primary astrocytes were treated with 20 μM BRC or DMSO (vehicle control) for 24 h, and then exposed t
24 h. The amount of TNF-α in the culture medium, which was released from the cells, was measured by ELISA. Data are expressed as mean ± SEM (n = 3). ** $p < 0.01$ by Student's
each corresponding control.

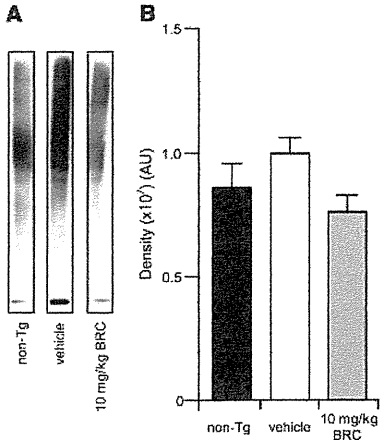

Supplementary Fig. 4. Effect of the BRC treatment on oxidative damage to tissue proteins. (A) Formation of protein carbonyl in the soleus muscle from non-Tg, vehicle-treated ALS(S 10 mg/kg BRC-treated ALS(SOD1^{H46R}) mice at a late symptomatic stage (21–22 weeks of age) was detected by immunoblotting using anti-dinitrophenyl (DNP) antibody. (B) Quantita protein carbonyl groups in non-Tg, vehicle-treated ALS(SOD1^{H46R}), and 10 mg/kg BRC-treated ALS(SOD1^{H46R}) mice are shown. Data are expressed as mean ± SEM (n = 4).

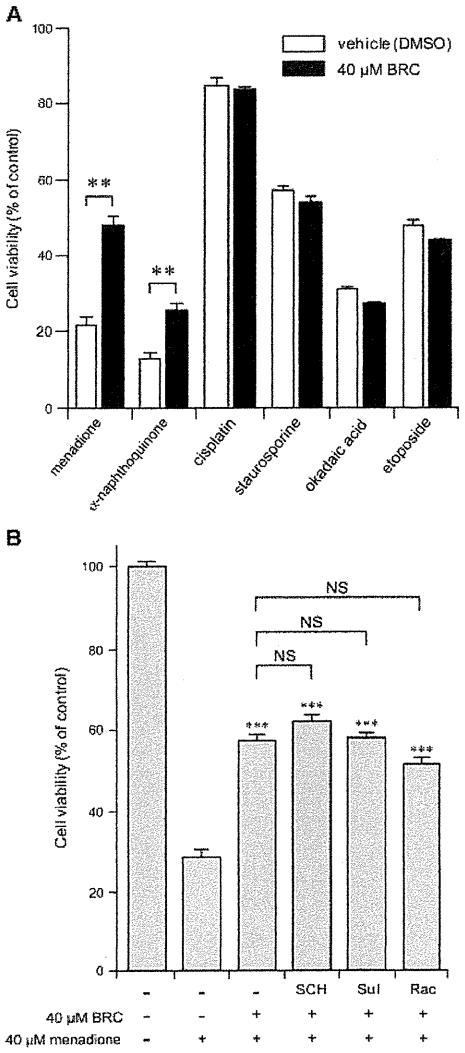

Supplementary Fig. 5. (A) Effect of BRC on cell death induced by various cytotoxic insults. Differentiated SH-SY5Y cells were treated with 40 µM BRC. After 24 h, cells were exposed cytotoxins; menadione and α-naphthoquinone (free radical generating compound), cisplatin (DNA-damaging reagent), staurosporin (kinase inhibitor), okadaic acid (phosphatase inhib (topoisomerase II inhibitor). Cell viability was measured with the Alamar blue assay (Invitrogen). Data are expressed as mean ± SEM (n = 3). Statistical analysis was performed using $p < 0.01$, versus each corresponding vehicle. (B) Effect of dopamine receptor antagonists on the BRC-mediated neuroprotection. Differentiated SH-SY5Y cells were preincubated for SCH23390 (SCH; 20 µM) (n = 4), Sulpiride (Sul; 20 µM) (n = 4), or Raclopride (Rac; 20 µM) (n = 4), followed by the treatment with 40 µM BRC. After 24 h, cells were exposed to 40 µ radical inducer) for 4 h. Cell viability was measured with the Alamar blue assay (Invitrogen). Percentages relative to non-treated cells are shown. Data are expressed as mean ± SEM cells exposed to menadione alone and BRC followed by menadione, n = 12). *** $p < 0.0001$ by one-way ANOVA with Scheffe's *post hoc* test compared with cells exposed to menadic significant.

IV. 添付資料

資料１

臨床研究プロトコール

日本語版

NDDPX08を用いた筋萎縮性側索硬化症の機能改善および安全性に関する検討

Study of efficacy and safety of NDDPX08 in ALS patients

研究組織名

東海大学付属病院

研究代表者　池　田　穣　衛

住所　〒259-1193 伊勢原市下糟屋 143

電話番号　0463-93-1121　内線 2566

FAX 番号　0463-91-4993

E-mail Address :　jeikeda3@is.icc.u-tokai.ac.jp

制作２００８年１１月１８日　第１版

改訂２００９年　２月　６日 第１．１版

改訂２００９年　４月　９日 第１．２版

改訂２００９年　４月２２日 第１．３版

改訂２００９年１０月２０日　第２版

改訂２０１０年　３月　４日 第２．１版

改訂２０１０年　８月　１０日 第２．２版

秘密保全について

本臨床研究計画書は、本臨床研究に関わる、
審査委員会
臨床研究責任者
臨床研究責任医師
臨床研究分担医師
臨床研究協力者
東海大学医学部長
東海大学医学部付属病院長
および本臨床研究の実施に関与する東海大学医学部および
その付属病院の各部署に限定して提供される秘密情報として
取り扱うこととする。